Bulgarian Chemical Communications, Volume 51, Issue 3 (pp. 439- 444) 2019 DOI: 10.34049/bcc.51.3.5142

Photocatalytic behavior of ZnSe-TiO_2 composite for degradation of methyl orange dye under visible light irradiation

N. G. Kostova*[1], M. Achimovicova[2], M. Fabian[2]

[1] *Institute of Catalysis, Bulgarian Academy of Sciences, Acad. G. Bonchev St., Bldg. 11, 1113 Sofia, Bulgaria*
[2] *Institute of Geotechnics, Slovak Academy of Science, 04001 Kosice, Slovakia*

Received April 22 2019; Revised June 14, 2019

In the present study we report the preparation of ZnSe-TiO_2 composite *via* a two-step mechanochemical synthesis. ZnSe with 10 nm crystallite size was mechanochemically synthesized in industrial mill using zinc and selenium as precursors. The composite material was synthesized in laboratory high-energy ball mill. The synthesized material was characterized by means of various techniques including X-ray powder diffraction (XRD) and UV-vis diffuse reflectance spectra (DRS). The results revealed a composite formation. The calculated band gap was 2.3 eV. The prepared structured materials were employed as photocatalysts for the degradation of methyl orange (MO) under visible light illumination. The results exhibited higher photocatalytic efficiency over ZnSe-TiO_2 composite material in comparison with those of pure ZnSe and TiO_2, which might be attributed to the high surface area and the synergetic effect between zinc selenide and titania. It was established that the reaction was of pseudo-first order. A possible mechanism was proposed. The mechanochemically synthesized ZnSe-TiO_2 composite material exhibited stability in photocatalytic activity after four cycles.

Keywords: mechanochemistry, photocatalysis, ZnSe, methyl orange, dye

INTRODUCTION

Heterogeneous photocatalysis using semiconductors has received attention because of its potential in solving environmental problems [1]. This method is based on the production of electron-hole pairs by illumination with suitable energy light of semiconductor materials. Nanosized particles have unique physical and chemical properties that make them applicable in the photocatalytic process [2, 3]. The photocatalytic degradation of toxic compounds (dyes, pesticides, etc.) using the photo-catalytic materials in an aqueous medium depends on the band gap, surface area, amount of catalyst, etc. Different metal oxides [4] and sulfides [5] have been employed as photocatalysts for dyes photodegradation. TiO_2 is one of the best photo-catalysts for environmental applications because of its strong oxidizing and reducing ability, low cost and availability. However, TiO_2 only responds to UV light due to its wide band gap, which restricts its applications [6]. Many attempts have been devoted to improving the visible-light photocatalytic activity of TiO_2. Recently, studies have reported various methods of coupling TiO_2 to a narrow-band gap semiconductor to enhance the photocatalytic effi-ciency under visible light irradiation. Coupling semiconductors with different band gap structures could enhance the electron-hole separation and increase the charge carrier lifetime, which conse-quently enhances the photodegradation efficiency [7].

Metal chalcogenides semiconductors have narrow band gap and show good photocatalytic activity under visible light illumination [8, 9]. ZnSe is a type of II-VI semiconductor with a band gap of 2.67 eV at room temperature, which can be excited by visible light [10]. The chalcogenide semicon-ductors have been fabricated by different methods. Mechanochemical method is one of the powerful techniques for synthesis of sulfides. Mechanochemical synthesis of various chalcogenide semiconductors has been described in several works [11-15]. This preparation route concerns the solid state reactions induced by mechanical energy [16]. Gock and co-authors have described the industrial production of nanoscale metal sulfides by means of reactive grinding [17]. Recently, our research group reported the mechanochemically synthesized CdS-TiO_2 and ZnS-TiO_2 nanocomposites for use in photocatalytic applications [18, 19]. The coupling of CdS to TiO_2 may reduce the band gap of CdS-TiO_2 nanocomposites, thus facilitating the absorption of visible light [18].

The main aim of present research is to investigate photocatalytic properties of the ZnSe-TiO_2 composite prepared by mechanochemical synthesis. We chose the toxic and mutagenic methyl orange dye as a target pollutant because it is stable under visible light irradiation [20]. The photo-catalytic performance was evaluated by the removal efficiency of methyl orange (MO), involving the degradation.

* To whom all correspondence should be sent
E-mail: nkostova@ic.bas.bg

Moreover, the photocatalytic degrada-tion kinetics and mechanism, so as the reusability of ZnSe-TiO_2 photocatalyst were studied.

EXPERIMENTAL

Materials

Chemicals used for the synthesis were zinc (97% mean particle size 39 μm, Ites, Slovakia) and selenium powders (99.5%, mean particle size 46 μm, Aldrich, Germany) and commercial TiO_2 P 25 (Degussa, Holland). They were applied as received without further purification. Methyl orange was used in this study as a representative azo dye for the assessment of photocatalyst dye degradation ability. Methyl orange is an anionic azo dye which also works as a pH indicator (chemical formula $C_{14}H_{14}N_3NaO_3S$; chemical name 4-[4-(Dimethyl-amino)phenylazo]benzenesulfonic acid sodium salt; M 327.33; orange colour; pH 4.4).

Powder preparation

The ZnSe-TiO_2 composite was prepared by a two-step method. Firstly, the mechanochemical synthesis of ZnSe nanoparticles was performed by milling of the mixture of zinc and selenium powders in an industrial eccentric vibratory mill ESM 656-0.5 ks (Siebtechnik, Germany), according to the reaction: Zn + Se = ZnSe. The reaction is thermo-dynamically possible because of the negative value of enthalpy change $\Delta H^0_{298} = -159$ kJ mol^{-1}.

The following conditions were used for mecha-nochemical synthesis in the industrial eccentric vibratory mill: chamber and balls – tungsten carbide, balls diameter 30 mm with a total mass of 17 000 g; rotation speed of motor – 960 rpm, the amplitude of the inhomogeneous vibrations – 20 mm and milling time 15 min; loading of the mill – material of 5 L, milling mass of Zn – 45.3 g, mass of Se – 54.7 g, milling atmosphere – Argon,. After that as prepared ZnSe powder was milled together with TiO_2 P 25 Degussa at a ratio of 1:4 for 30 min in a high-energy planetary ball mill at 500 rpm.

Characterization methods

X-ray diffraction measurements were carried out using a X`Pert diffractometer (Philips, Netherlands), working in the geometry with CuKα radiation. The JCPDS PDF database was utilized for phase identification. The crystallite size values of the products were calculated from (111) reflection using Scherrer's equation [21].

The specific surface area was determined by the low-temperature nitrogen adsorption method using a Gemini 2360 sorption apparatus (Micromeritics, USA).

The diffuse reflectance UV-vis spectra for eva-luation of photophysical properties were recorded in the diffuse reflectance mode and transformed to absorption spectra through the Kubelka-Munk func-tion. A Thermo Evolution 300 UV-vis Spectropho-tometer (ThermoScientific, USA), equipped with a Praying Mantis device was used. The reflectance data were obtained as a relative percentage of reflectance to a no-absorbing material (spectralon) which can optically diffuse light.

The photocatalytic activity of all samples was measured by means of methyl orange (MO) photo-degradation. The concentration of MO in reaction solution was 10 mg L^{-1}. In a typical measurement, 100 mL of aqueous suspension of MO and 100 mg of the photocatalyst were placed in the semi-batch suspension photocatalytic reactor under constant air flow. The obtained suspension was subjected to stirring in the dark for 30 min to obtain the adsorption-desorption equilibrium between the photocatalysts and organic pollutant. Then, the mixed suspension was kept under visible light illumination by halogen lamp (illumination intensity 8.9 $mW \cdot cm^{-2}$). All experiments were performed at a constant stirring rate of 400 rpm at room tempera-ture. At a given time interval the illumination was stopped, 6 mL of suspension was sampled and centrifuged to remove the photo-catalyst. The tem-poral concentration of MO was estimated at 463 nm using a SPEKOL 11 (Carl Zeiss Jenna, Germany) spectrophotometer. Each analyzed aliquot sample was returned to the reaction mixture after the spectrophotometric measurement for further operation under constant volume. The illumination was switched on again.

RESULTS AND DISCUSSION

Fig. 1 shows the X-ray powder diffraction pat-tern of the mechanochemically synthesized product formed after 15 min of milling in the industrial vibratory mill. The XRD peaks at $2\theta = 27.3$, 45.2, and 53.6° were indexed as the (111), (220), and (331) planes of cubic ZnSe. It is worth to note that the traces of the un-reacted Zn phase were also detected. The XRD analysis of the mechano-chemically synthesized ZnSe product confirmed its nanocrystalline nature. Calculated crystallite size using the reflection of ZnSe (111) plane was 10 nm.

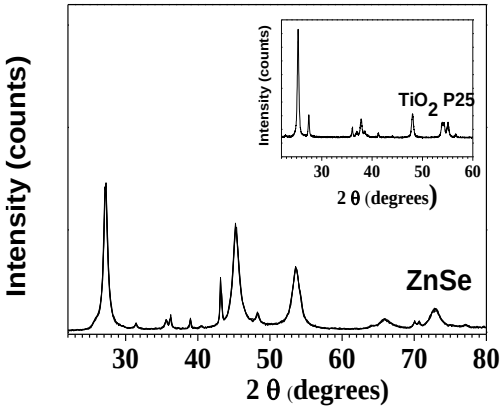

Fig. 1. XRD patterns of mechanochemically synthesized ZnSe, ZnSe-TiO_2, and commercial TiO_2 P25 (inset).

The specific surface area of mechanochemically synthesized ZnSe was 2.33 m^2g^{-1} and that of the commercial TiO_2 P25 was 52 m^2g^{-1}. The mechanochemically synthesized ZnSe-TiO_2 composite possessed lower specific surface area (S_{BET} = 40 m^2g^{-1}) indicating that milling resulted in deterioration of the porous structure. The reduction of S_{BET} value of TiO_2 upon milling was also reported in [22].

The optical properties of semiconductors were investigated by UV-visible diffuse reflectance spectroscopy. The absorbance data were obtained from diffuse reflectance data by the Kubelka-Munk method and the results are shown in Fig. 2. The absorption edge of TiO_2 P25 is located only in the UV region.

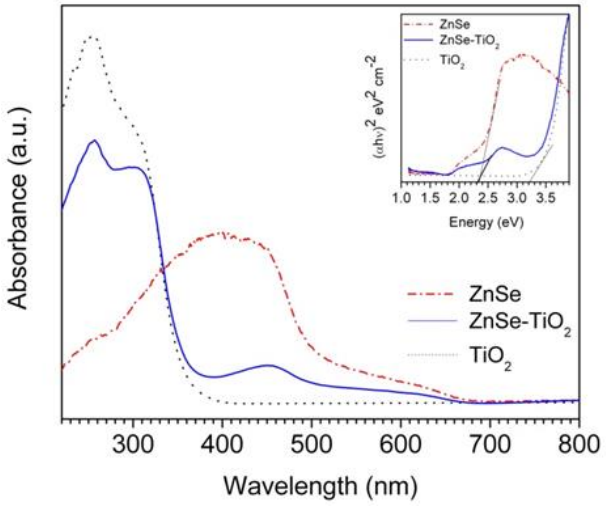

Fig. 2. UV-vis DRS of the TiO_2, ZnSe and ZnSe-TiO_2 samples. The inset shows plot of $(h\nu)^2$ vs. photon energy for the band gap energy.

The experimental result indicated that the mechanochemically synthesized ZnSe powder possessed good visible light absorption. This result is in accordance with the brownish colour of the sample. It can be seen from Fig. 2 that after the coupling of mechanochemically synthesized ZnSe with TiO_2 P25, a well defined absorbance in the visible light region was observed in the optical properties of the ZnSe-TiO_2 composite and it was significantly enhanced compared to pure TiO_2.

The band gap energy (E_g) was calculated by a modified Kubelka-Munk function, F(R) [23]. $F(R) = (1-R)^2/2R = K/S$, where K and S are the absorption and scattering coefficients, respectively. The absorption coefficient α is related to the incident photon energy by means of the Tauc's equation [24] $\alpha h\nu = C(h\nu - E_g)^{1/2}$, where C is a proportionality constant and $h\nu$ is the proton energy. The band gap of mechanochemically synthesized ZnSe was estimated by plotting $(\alpha h\nu)^2$ vs. hν as shown in inset of Fig. 2 and extrapolating the linear portion near the onset of absorption edge to the energy axis. The band gap of mechanochemically synthesized ZnSe is 2.33 eV, which is narrower than that of bulk ZnSe (2.67 eV). Compared to TiO_2 P25, the band gap value of ZnSe-TiO_2 is smaller, indicating that the absorption ability of ZnSe-TiO_2 can be extended by coupling ZnSe to TiO_2.

The photocatalytic performance of the samples was evaluated under visible light irradiation using methyl orange azo dye as a model contaminant. Fig. 3a shows MO adsorption on the ZnSe, ZnSe-TiO_2 and TiO_2 samples measured at regular time intervals in the course of the dark period. The adsorption on the surface of the particles is fast during the initial 5 minutes. After that, there is a slight increase in adsorption until equilibrium is reached after 30 min of contact time. The adsorption capacities are determined using the equation: $Q = (C_0\text{-}C).V/m$, where C_0 and C are the initial and current concentrations, respectively, V is the volume of the solution; m is the mass of the catalyst. The adsorption capacity of the photocatalysts in respect of MO dye after 30 min contact time without irradiation follows the line ZnSe < ZnSe-TiO_2 < TiO_2. The results show that the MO adsorption capacity of mechanochemically synthesized ZnSe is very small.

Fig. 3a inset indicates the absorption spectra of MO solution with the sample ZnSe-TiO_2 during visible light illumination. MO has an important peak at 463 nm that was monitored for investigating the MO degradation. Increasing illumination time, the absorption peak intensity decreased indicating photodecolourization of MO. Change in the solution colour also indicates and confirms the photodegradation of MO dye by ZnSe-TiO_2. The loss of absorbance was due to the destruction of the dye –N=N– chromophore group.

As shown in Fig. 3b, almost no MO degradation could be observed under visible light irradiation in the absence of a photocatalyst, suggesting that degradation by direct photolysis could be ignored. TiO_2 P25 exhibits only 4% photocatalytic efficiency under visible light irradiation which can be attributed to its wide 3.2 eV band gap. Among the mechanochemically prepared samples, ZnSe-TiO_2 composite shows the highest photocatalytic activity with 80% MO degradation in 120 min (Fig. 4). The photocatalytic activities decreased in the order, ZnSe-TiO_2 > ZnSe > TiO_2.

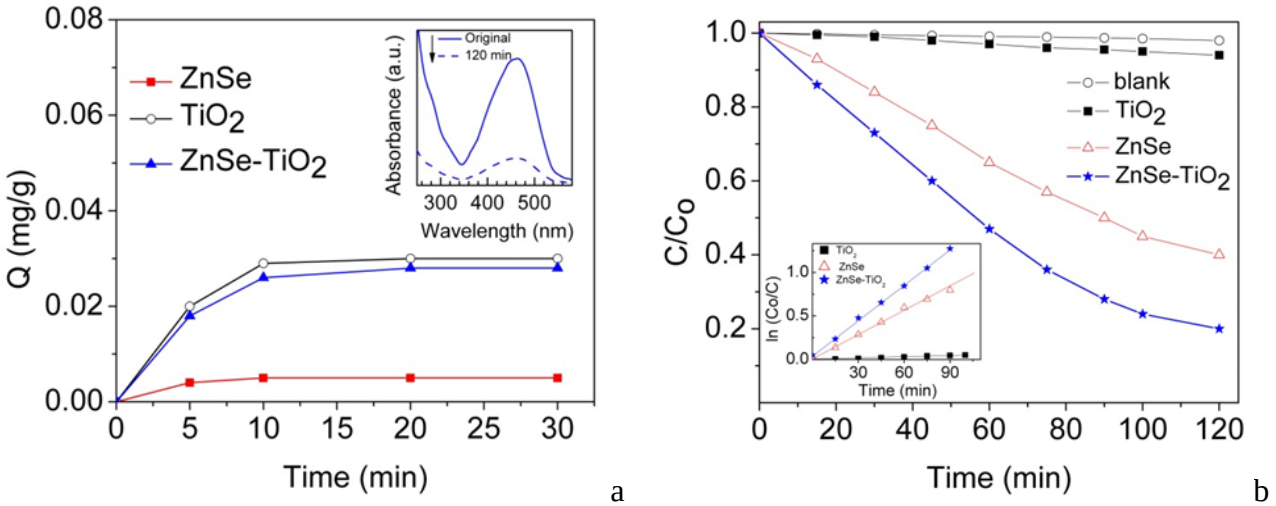

Fig. 3. a – Comparison of MO adsorption in dark on TiO_2, ZnSe, and ZnSe-TiO_2 samples and absorption spectra of original MO and after irradiation for 120 min in presence of ZnSe-TiO_2 composite (inset).; b – Degree of MO degradation as a function of irradiation time of blank experiment (without photocatalyst), TiO_2, ZnSe, and ZnSe-TiO_2 samples; kinetic curves of photocatalytic degradation of MO under visible light irradiation (inset).

The photocatalytic degradation process involving MO in aqueous solution can be interpreted through a modified Langmuir-Hinshelwood kinetic model. The reaction kinetics can be expressed as $\ln(C_0/C) = kt$, where C_0 and C are the initial and actual concentration of MO, respectively, and *k* is the apparent rate constant of the degradation. The photodegradation of MO under visible light irradiation, catalyzed by the mechanochemically synthesized ZnSe and ZnSe-TiO_2 fits pseudo-first order reaction (Fig. 3b inset). The rate constant of MO photocatalytic degradation over suspended semiconductor materials irradiated with visible light decreases in the following order: ZnSe-TiO_2 > ZnSe > TiO_2 (Fig. 3b inset). Compared with mechano-chemically synthesized ZnSe the ZnSe-TiO_2 composite showed a 1.61-fold increase in the rate constant of MO degradation under visible light irradiation. The higher value of the rate constant of MO degradation with ZnSe-TiO_2 can be explained in terms of an increased rate of charge carriers (h^+ and e^-) separation in the photoexcited composite as a dominating kinetic factor.

The reusability of the ZnSe was also studied. Recycling experiments of ZnS-TiO_2 and ZnSe for MO photocatalytic degradation under visible light irradiation were carried out and the results are presented in Fig. 5. After each examination, the ZnSe was immersed into fresh MO azo dye solution of the same concentration for another cycle. This process was repeated 4 times. There was no signi-ficant change in the efficiency of ZnSe photocatalyst even after four runs. This shows the reusability and stability of the mechanochemically prepared ZnSe photocatalyst.

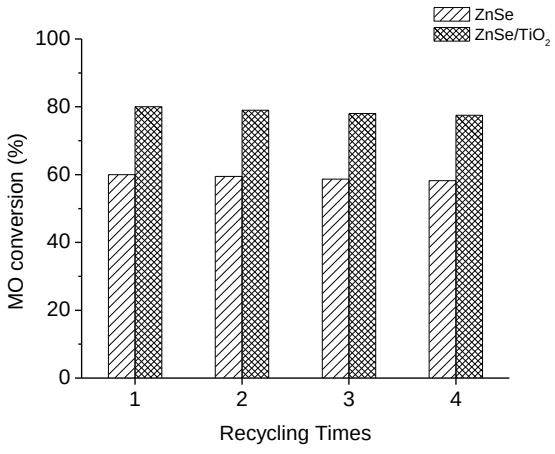

Fig. 4. The reusability diagrams of mechanochemically synthesized ZnSe and ZnSe-TiO_2 for 4 runs.

Methyl orange azo dye is characterized by nitrogen double bond (–N=N–) that is usually attached to radicals of aromatic groups. The azo bond is the most active bond in the azo dye molecules and can be oxidized by a positive hole or hydroxyl

radical or reduced by an electron in the conduction band. The cleavage of –N=N– bond leads to the decolonization of dye. The energy of the band gap of the mechanochemically synthesized ZnSe-TiO_2 estimated from the DRS is 2.33 eV. It is helpful to generate higher electron and hole pairs. When the ZnSe-TiO_2 composite is irradiated with visible light, it results in the excitation of electrons (e^-) into the conduction bands (CB) of both TiO_2 as well as ZnSe semiconductors thereby leaving the holes (h^+) behind in their valence bands (VB). Owing the suitable positions of conduction band and valence band, the electrons from the CB of ZnSe are transferred to conduction band of TiO_2, whereas the holes from TiO_2 valence band are thereby trans-ferred to the VB of ZnSe (Fig. 5). The holes are subsequently trapped by absorbed H_2O on the surface of ZnSe to generate highly reactive hydroxyl radicals (•OH). The conduction band electrons may react with dissolved oxygen to to form a superoxide anion radical ($•O_2^-$). The radicals including •OH and $•O_2^-$ present strong oxidizing properties and are able to cause depredation of MO [8].

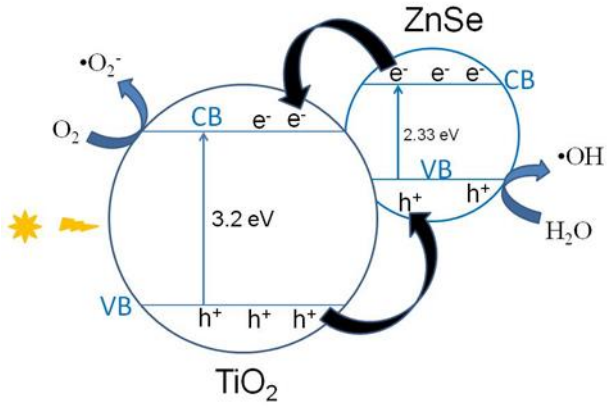

Fig. 5. The suggested mechanism for charge transfer of the photogenerated electrons and holes on mechano-chemically synthesized ZnSe-TiO_2 under visible light irradiation.

To understand the mechanism of MO degradation on ZnSe-TiO_2 composite, it is necessary to detect which reactive species play a major role in the photocatalytic degradation process. During photodegradation of MO over ZnSe-TiO_2 composite, the h^+, •OH, and $•O_2^-$ are eliminated by adding EDTA (h^+ scavenger), TBA - *tert*-butyl-alcohol (•OH scavenger) and BQ - *p*-benzoquinone ($•O_2^-$ scavenger) into the reaction solution, respectively. Fig. 6 shows the MO photodegradation over ZnSe-TiO_2 composite in the absence and presence of scavengers. The decrease of the removal rate in the presence of scavengers presents the following trend: BQ > EDTA> TBA. Hence, the superoxide radical is the main reactive species during photocatalytic degradation of MO. Thus, it was reasonable to conclude that $•O_2^-$, h^+, and •OH as oxidation species were indeed photogenerated on catalyst surface and responsible for the photo-catalytic degradation of MO over mechanoche-mically synthesized ZnSe-TiO_2 composite.

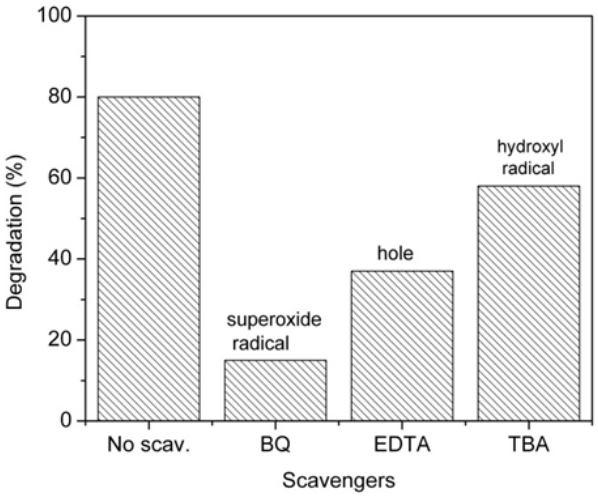

Fig. 6. Effect of different scavengers on MO photo-degradation under visible light over the mechano-chemically synthesized ZnSe-TiO_2 composite.

The mechanochemically synthesized ZnSe was demonstrated as an effective, environmentally safe and recyclable photocatalyst under visible light. The good photocatalytic properties of ZnSe open a new region of possible applications. The main advantage of the mechanochemically synthesized sample is that their band gaps is about 2.33 eV in comparison to TiO_2 (3.2 eV), which leads to the observed higher photocatalytic activity of ZnSe and ZnSe-TiO_2 composite under visible irradiation.

CONCLUSIONS

The industrial vibratory mill has been proved as an effective reactor for solid state synthesis of ZnSe nanoparticles starting from zinc and selenium as reaction precursors. The final ZnSe material possesses the cubic crystal structure. ZnSe-TiO_2 composite has been successfully synthesized by mechanochemical route. The photocatalytic results exhibit higher efficiency of the composite in comparison with pure ZnSe and TiO_2 under visible light. The reaction is pseudo-first order. The mecha-nochemically synthesized ZnSe-TiO_2 composite was demonstrated as an effective, environmentally safe and recyclable photocatalyst.

Acknowledgements: *The present work was supported by the Bulgarian National Science Fund by project DNTS/Slovakia 01/2, Slovak Research and Development Agency APVV-18-0357 and „Research Centre of Advanced Materials and Technologies for Recent and Future Applications „PROMATECH", ITMS 26220220186, of the Operational Program "Research and Development" financed through European Regional Development Fund.*

REFERENCES

1. K. Daghrir, P. Drpgui, D. Robert, Ind. Eng. Chem. Res., **52**, 3581 (2013).
2. L. Pan, X. Liu, Z. Sun, C. Q. Sun, *J. Mater. Chem*. A, **1**, 8299 (2013).
3. M. N. Gancheva, P. M. Konova, G. M. Ivanov, L. I. Aleksandrov, R.I. Iordanova, A.I. Naydenov, *Bulg. Chem. Commun*., **50** Special issue, H 93 (2018).
4. V. Iliev D. Tomova, A. Eliyas, S. Rakovsky, M. Anachkov, L. Petrov, *Bulg. Chem. Commun.,* **47**, Special Issue C, 5 (2015).
5. M. Balaz, E. Dutkova, Z. Bujnakova, E. Tothova, N.G. Kostova, Y. Karakirova, J. Briancin, M. Kanuchova, *J. Alloys Comp*. **746**, 576 (2018).
6. O. Carp, C.L. Huisman, A. Reller, *Prog. Solid State Chem*., **32**, 33 (2004).
7. N. G. Kostova, M. Fabian, E. Dutkova, N. Velinov, Y. Karakirova, M. Balaz, *Bulg. Chem. Commun*., **50**, Special Issue H, 109 (2018).
8. K. Liu, L. Zhang, N. J. Ji, H. Liu, *Optoelectronics Adv. Mater. Rapid Commun*., **8**, 873 (2014).
9. C. Sun, Y. Gue, W. Wen, L. Zhao, *Optical Mate*r., **81**, 12 (2018).
10. D. Ayodhya, G. Veerabhadram, *Mater. Today Energy*, **9**, 83 (2018).
11. P. Balaz, M. Balaz, E. Dutkova, A. Zorkovska, J. Kovac, P. Hronec, J. Kovac Jr., M. Chaplovicova, J. Mojzis, G.Mojzisova, A. Eliyas, N. G. Kostova, *Mater. Sci. Eng. C*, **58**, 1016 (2016).
12. P. Balaz, M. Balaz, M. Achimovicova, Z. Bujnakova, E. Dutkova, *J. Mater. Sci.*, **52**, 11851 (2017).
13. M. Achimovicova, N. Daneu, E. Dutkova, A. Zorkovska, *Appl. Phys. A – Mater. Sci. & Process.*, **123** (3) Article Number 154 (2017).
14. M. Achimovocova, P. Balaz, Nanocrystalline metal selenides: Mechanochemical synthesis and utilizable properties, in: Milling Fundamentals, Processes and Technologies (M. Ramirez Ed.) pp. 71-122 (Book Chapter) ISBN-13, 978-1634830225, Nova Science Publishers, Inc. New York, 2015.
15. E. Dutkova, M. Caplovicova, I. Skorvanek, M. Balaz, A. Zorkovska, P. Balaz, L. Caplovic, *J. Alloys Comp.*, **745**, 863 (2018).
16. K. Assaker, B. Lebeau, L. Michelin, P. Gaudin, C. Carteret, L. Vidal, M. Bonne, J. L. Blin, *J. Alloys Comp*., **649,** 1 (2015).
17. M. Achimovicova, P. Balaz, J, Durisin, N. Daneu, J. Kovac, A. Satka, A. Feldhoff, E. Goch, *Intern. J. Mater. Res.*,**102**, 441 (2011).
18. N.G. Kostova, E. Dutkova, A. Eliyas, E. Stoyanova-Eliyas, M. Fabian, P. Balaz, *Bulg. Chem. Commun*., **47**, Special issue C pp.87 (2015).
19. N.G. Kostova, E. Dutkova, *Bulg. Chem. Commun*., **48**, Special Issues G, 161 (2016).
20. K. T. Chung, C. E. Cerniglia, *Mutat. Res.*, **277**, 201 (1992).
21. H. P. Kligg, L. E. Alexander, X-Ray Diffraction Procedures, Wiley, New York, 1954; P. Scherrer, Bestimmung der Grösse und der inneren Struktur von Kolloidteilchen mittels Röntgenstrahlen, Nachr Ges Wiss Göttingen, **26**, 98–100 (1918).
22. P. Dulian, M. Buras, W. Zukovski, *Polish J. Chem. Technol*. **18**, 68 (2016).
23. S. Valencia, J. M. Marin, G. Resrepo, *Open Mater. Sci. J.*, **4,** 9 (2010).
24. J. Tauc, R. Grigorovic, A. Vancu, *Phys. Status Solidi*, **15,** 627 (1966).